Control of Spin State by Ring Conformation of Iron(III) Porphyrins. A Novel Model for the Quantum-Mixed Intermediate Spin State of Ferric Cytochrome *c*′ from Photosynthetic Bacteria

Ru-Jen Cheng,*[,1a] Ping-Yu Chen,[1a] Pong-Ren Gau,[1a] Chun-Chia Chen,[1a] and Shie-Ming Peng[1b]

Contribution from the Department of Chemistry, National Chung-Hsing University, Taichung, Department of Chemistry, National Taiwan University, Taipei, Taiwan, ROC

Received July 17, 1996[⊗]

Abstract: (2,3,7,8,12,13,17,18-Octaethyl-5,10,15,20-tetraphenylporphinato)iron(III) chloride Fe^{III}(OETPP)Cl and (2,3,7,8,12,13,17,18-octamethyl-5,10,15,20-tetraphenylporphinato)iron(III) chloride Fe^{III}(OMTPP)Cl complexes have been synthesized and characterized by ^{1}H NMR and X-ray crystallography. Both molecules are severely nonplanar and assume saddle shapes in solid state. Variable-temperature ^{1}H NMR studies confirm that the conformational distortions are maintained in solution with $\Delta G^{\ddagger} = 15.8$ and 10.1 kcal/mol for ring inversion for Fe(OETPP)Cl and Fe(OMTPP)Cl, respectively. EPR ($g_{\perp} = 5.2-5.3$ at 77 K), magnetic moments ($\mu_{eff} = 4.7-5.2\ \mu_B$ at 300 K), and structural data ($Fe-N_p = 2.03$ Å, $Fe-Cl = 2.24-2.25$ Å) all indicate that unlike high-spin Fe^{III}(TPP)Cl and Fe^{III}(OEP)Cl ($S = 5/2$), Fe^{III}(OETPP)Cl and Fe^{III}(OMTPP)Cl these complexes are of the uncommon quantum-mixed $S = 5/2$, 3/2 intermediate-spin state. Saddle-shaped ring deformations lower the symmetries of the complexes into C_{2v}. Other than the nonaxial symmetric EPR spectra of both complexes, ^{1}H NMR spectrum of Fe^{III}(OETPP)Cl shows large asymmetry to the methylene proton shifts. Certain cytochromes *c*′ from photosynthetic bacteria reported to be of similar quantum-mixed intermediate-spin and showed EPR signals of rhombic symmetry have been noted to be with saddle-shaped deformations. These anomalous spin states and electronic structure asymmetry are ascribed to the ring deformation of the porphyrin macrocycle.

Introduction

Iron porphyrins serve many diverse functions in biological systems. It may change from an oxygen carrier to an oxygen activation catalyst just by protein fine-tuning of the structure around the heme. Biological activities of hemoproteins can be modulated by the following protein-induced constraints to heme prothetic groups: (i) providing axial ligands from amino acid residues; (ii) forming hydrogen-bonding either to axial ligands or to porphyrin side chains; (iii) forming a hydrophobic pocket around active site; and (iv) steric interactions that constrain the orientation of axial ligand plane[2,3] or distort the shape of porphyrin macrocycle.[4] Extensive work on model systems and hemoproteins has established that the ligands coordinated to the axial sites of the metal ion are a strong determinant of the electronic structure and function of the chromophore.[5] On the other hand, it has been suggested recently that nonplanar conformations of tetrapyrrole prosthetic groups may play a critical role in modulating their physicochemical properties.[4,6] In particular, nonplanar distortions of the macrocycle which result from steric interactions among the peripheral substitutions have been investigated in order to understand the functional consequences of similar distortions observed for the tetrapyrrole derivatives in various proteins.[7,8]

2,3,7,8,12,13,17,18-Octaethyl-5,10,15,20-tetraphenylporphyrin (OETPP) may be considered to be a structural hybrid of the well-studied 2,3,7,8,12,13,17,18-octaethylporphyrin (OEP) and 5,10,15,20-tetraphenylporphyrin (TPP), which has been found to be severely distorted into a saddle-shape both in solid state and in solution. The consequences of saddle deformation on the properties of OETPP are significant and are reflected in the red-shifted optical spectrum, diminished fluorescence, ease of oxidation, and dramatically increased basicity.[7] Because of their biological relevance and wealth of comparative data, octaethyltetraphenylporphyrin provides an excellent opportunity to explore the subtle effects of ring conformation on the properties of coordinated metal ions in porphyrin complexes. The methyl analog OMTPP will also be reported for comparison.

Experimental Section

Synthesis. Porphyrin free bases $OETPPH_2$ and $OMTPPH_2$ were prepared from benzaldehyde and the corresponding pyrroles following literature procedures.[7] The *p*-methyl substituted $OETPPH_2$ ($OETTPH_2$) and phenyl-deuterated $OETPPH_2$ ($OETPPH_2$-d_{20}) derivatives were prepared in similar fashions starting with *p*-tolylaldehyde and benzaldehyde-d_5, respectively. Iron was inserted using ferrous chloride tetrahydrate in DMF as described earlier.[9]

Fe(OETPP)Cl was prepared as above, using CH_2Cl_2/hexane for recrystallization. $\lambda_{max}(CH_2Cl_2)$: 396 nm (ϵ 6.28 × 10^4), 444 nm (ϵ 5.84 × 10^4).

⊗ Abstract published in *Advance ACS Abstracts,* February 15, 1997.

(1) (a) National Chung-Hsing University. (b) National Taiwan University.

(2) Scheidt, W. R.; Geiger, D. K.; Hayes, R. G.; Lang, G. *J. Am. Chem. Soc.* **1983**, *105*, 2625−2632.

(3) Walker, F. A.; Huynh, B. H.; Scheidt, W. R.; Osvath, S. R. *J. Am. Chem. Soc.* **1986**, *108*, 5288−5297.

(4) Barkigia, K. M.; Chantranupong, L.; Smith, K. M.; Fajer, J. *J. Am. Chem. Soc.* **1988**, *110*, 7566−7567.

(5) Scheidt, W. R.; Reed, C. A. *Chem. Rev.* **1981**, *81*, 543−555.

(6) Barkigia, K. M.; Gottfried, D. S.; Boxer, S. G.; Fajer, J. *J. Am. Chem. Soc.* **1989**, *111*, 6444−6446.

(7) Barkigia, K. M.; Dolores Berber, M.; Fajer, J.; Medforth, C. J.; Renner, M. W.; Smith, K. M. *J. Am. Chem. Soc.* **1990**, *112*, 8851−8857.

(8) Cheng, R.-J.; Chen, Y.-R.; Chuang, C.-E. *Heterocycles* **1992**, *34*, 1−4.

(9) Sparks, L. D.; Medforth, C. J.; Park, M.-S.; Chamberlain, J. R.; Ondrias, M. R.; Senge, M. O.; Smith, K. M.; Shelnutt, J. A. *J. Am. Chem. Soc.* **1993**, *115*, 581−592.

S0002-7863(96)02474-2 CCC: $14.00

Table 1. Crystal Data, Details of Intensity Measurements, and Structure Refinements for Fe(OETPP)Cl and Fe(OMTPP)Cl

	Fe(OETPP)Cl	Fe(OMTPP)Cl
empirical formula	$C_{60}H_{60}N_4FeCl{\cdot}2CH_2Cl_2$	$C_{52}H_{44}N_4FeCl{\cdot}CH_2Cl_2$
fw	1098.32	901.17
crystal system	monoclinic	monoclinic
space group	$P2_1/c$	$P2_1/c$
temp, K	298	298
a, Å	20.182(5)	16.314(3)
b, Å	19.222(4)	12.504(3)
c, Å	15.380(3)	22.767(5)
β, deg	103.739(20)	94.92(3)
V, Å^3	5795.7(22)	4626.9(17)
Z	4	4
crystal size, mm	0.50 × 0.50 × 0.60	0.05 × 0.50 × 0.50
color of crystal	indigo	indigo
D_{calcd}, g cm^{-3}	1.259	1.294
μ, cm^{-1}	5.315	4.185
radiation	Mo Kα	Mo Kα
$F(000)$	2304	1879
2θ range, deg	16.40−25.08	12.00−20.10
scan type	$\theta/2\theta$	$\theta/2\theta$
scan width, deg	$2(0.80 + 0.35 \tan \theta)$	$2(0.80 + 0.35 \tan \theta)$
scan speed, deg/min	3.30−8.24	2.06−5.50
transm range	0.908; 1.00	0.812; 1.00
no. of unique reflns	7570	6034
no. of reflns obsd[a]	4176	3136
computation	NRCSDP-VAX	NRCSDP-VAX
soln method	heavy atom	heavy atom
no. of params	639	550
R	0.064	0.064
R_w	0.060	0.058
goodness of fit, S[b]	1.93	2.13

[a] $I > 2\sigma(I)$. [b] $S = [\sum\omega(F_o - F_c)^2/(\text{no. of reflns} - \text{no. of params})]$.

Fe(OMTPP)Cl was prepared as above, using CH_2Cl_2/hexane for recrystallization. $\lambda_{max}(CH_2Cl_2)$: 396 nm (ϵ 5.98 × 10^4), 436 nm (ϵ 5.31 × 10^4).

Physical Measurement. ^{1}H NMR spectra were recorded on a Varian Gemini-200 or VXR-300 spectrometer. Electronic spectra were measured with Cary-3E spectrophotometer. EPR spectra were recorded at the X band with a Brüker spectrometer. Magnetic susceptibilities were measured in solution with use of the Evans technique or in solid state with QUANTUM DESIGN MPMS SQUID magnetometer operating at 3000 G. The diamagnetic susceptibilities of the porphyrin ligand and axial ligand were corrected by Pascal's rule.

Crystallography. Crystals of Fe(OETPP)Cl and Fe(OMTPP)Cl suitable for structure determinations were grown by slow diffusion of hexane into a solution of the metalloporphyrin in dichloromethane under air and were sealed with epoxy resin. Cell parameters were determined on a Nonius CAD-4 diffractometer by a least-squares treatment. Neutral atom scattering factors were taken from the International Tables for X-ray Crystallography.[10] Calculations were performed by using the NRCC SDP VAX package.[11]

Crystal data for Fe(OETPP)Cl and Fe(OMTPP)Cl, together with details of the X-ray diffraction experiments, are given in Table 1. Using C_α and C_β to denote the respective α and β-carbon atoms of a pyrrole ring, C_m for *meso*-carbon, and C_ϕ for a phenyl carbon atom that is bonded to the core, the average bond lengths and angles involving the porphyrin core and the coordination sphere of iron atom may be found in Table 2. Tables of final fractional atomic coordinates and anisotropic thermal parameters for the non-hydrogen atoms and final positional parameters for the hydrogen atoms are included in the Supporting Information.

Results

Crystal Structure. The projection of the structures and the atom-labeling schemes of Fe(OETPP)Cl and Fe(OMTPP)Cl are presented in Figure 1. It clearly shows the five-coordinate nature of the complexes. The extreme nonplanar nature of the porphyrin cores is evident in the perspective view of the isolated molecules shown in Figure 2. Each pyrrole ring with its β-alkyl substituents displaced alternately up and down, and the phenyl rings are rotated into the macrocycle plane to minimize contacts between the substituents. Formal diagrams of the porphyrin cores of Fe(OETPP)Cl and Fe(OMTPP)Cl are shown in Figure 3, in which we display the perpendicular displacement of each atom from the mean plane of the 24-atom core. Note that C_β atoms of adjacent pyrrole rings are alternately displaced above and below the macrocycle planes by 1.15 ± 0.11 and 1.05 ± 0.10 Å, respectively. The average dihedral angles between the mean porphyrin planes and pyrrole rings are 29.8° for Fe^{III}(OETPP)Cl and 26.5° for Fe^{III}(OMTPP)Cl. Also shown in the formal diagrams are the Fe−N_p bond distances. There is an interesting two long and two short pattern of Fe−N_p bond distances, where the long bonds correlate with the pyrrole rings tilting away from the central metal (*vide infra*).

Table 2. Comparisons of Selected Average Bond Lengths and Angles in Fe(OETPP)Cl and Fe(OMTPP)Cl with the Values in Fe(TPP)Cl

	Fe(OETPP)Cl	Fe(OMTPP)Cl	Fe(TPP)Cl[a]
	Distances, Å		
M−Cl	2.2418(23)	2.24(3)	2.211(1)
M−N	2.031(5)	2.034(6)	2.070(9)
C_α−N	1.386(7)	1.387(9)	1.383(5)
C_α−C_β	1.449(9)	1.445(10)	1.432(6)
C_β−C_β	1.360(9)	1.360(11)	1.343(6)
C_α−C_m	1.405(8)	1.399(11)	1.394(5)
C_m−$C_ø$	1.524(8)	1.495(10)	1.499(6)
	Angles, deg		
NMCl	103.2(16)	103.17(19)	103.7(1)
NMN	87.13(19)	87.18(22)	86.8(1)
$C_\alpha NC_\alpha$	106.18(5)	106.3(6)	105.8(3)
MNC_α	122.8(4)	124.1(5)	126.5(3)
$NC_\alpha C_m$	121.5(5)	122.0(7)	125.9(4)
$NC_\alpha C_\beta$	109.4(5)	109.3(6)	110.1(4)
$C_\beta C_\alpha C_m$	128.8(5)	128.2(7)	124.5(4)
$C_\alpha C_m C_\alpha$	123.0(5)	123.5(7)	124.1(4)
$C_\alpha C_\beta C_\beta$	107.2(5)	107.3(6)	107.5(4)

[a] From ref 12.

As expected for saddle deformations, the dihedral angles of the phenyl rings with the mean porphyrin planes are smaller than normally observed for planar macrocycles. The average values are 44.9° and 47.1° for Fe(OETPP)Cl and Fe(OMTPP)Cl, respectively. The orientations of the phenyl groups appear to depend upon interactions of the *ortho*-phenyl hydrogens with the adjacent pyrrole hydrogens; they all tilt toward the throughs of the saddle. It is clear from these structural characteristics that the peripherally crowded iron porphyrins are severely nonplanar and assume saddle shapes with Fe(OETPP)Cl more deformed than Fe(OMTPP)Cl.

Unlike Fe(OEP)Cl and Fe(TPP)Cl, of which the present compounds are hybrids, Fe(OETPP)Cl and Fe(OMTPP)Cl are strikingly nonplanar and exhibit severe saddle shapes. A comparison of some average bond distances and bond angles for Fe(OETPP)Cl, Fe(OMTPP)Cl, and Fe(TPP)Cl[12] is shown in Table 2. It is not surprising to find that excluding those bond lengths related to the metal atom (*vide infra*), bond lengths in the macrocycles are insensitive to the crowded periphery. The effects of the adjacent alkyl and phenyl groups are mainly reflected in the bond angles. As the pyrroles tilt to prevent unfavorable contacts between substituents, the C_β−C_α−C_m angles increase with a concomitant decrease in the N−C_α−C_m

(10) *International Tables for X-ray Crystallography*; Kynoch Press: Birmingham, 1974; Vol. IV.

(11) Gabe, E. J.; Lee, F. L. *Acta Crystallogr.* **1981**, *A37*, C339.

(12) Scheidt, W. R.; Finnegan, M. G. *Acta Crystallogr.* **1989**, *C45*, 1214−1216.

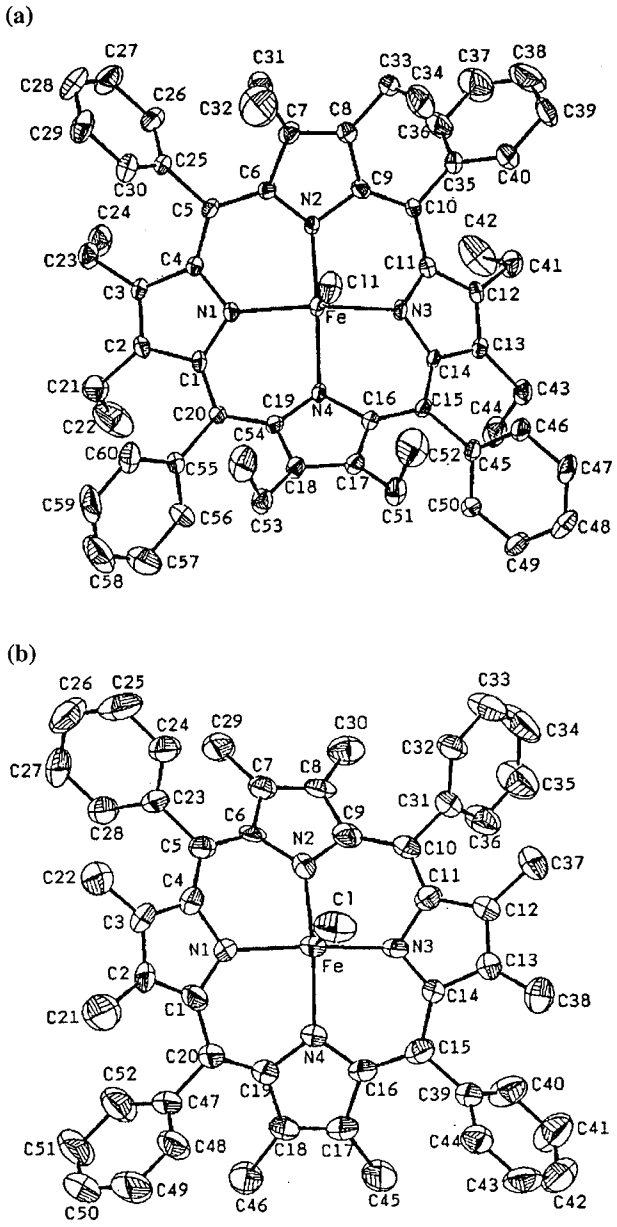

Figure 1. The projection of the structures and the atom-labeling schemes of (a) Fe(OETPP)Cl and (b) Fe(OMTPP)Cl. Hydrogens are omitted for clarity.

and M−N−C_α angles. The bond angle changes for OETPP are consistently larger than that for OMTPP. The remainder of the angles in both structures are essentially unperturbed.

Proton NMR Spectroscopy. Variable-temperature proton NMR spectra of Fe(OETPP)Cl taken in $C_2D_2Cl_4$ is typical of a paramagnetic species (Figure 4). All the resonances are assigned based on the relative intensities and line widths and further confirmed by methyl substitution and Fe(OETPP)Cl-d_{20} with deuterium-labeled at phenyl substituents. It is interesting to find that there are four peaks corresponding to the methylene protons of the ethyl substituents at low temperature. Diastereotopic methylene protons in five coordinated metalloporphyrins should give two sets of resonances instead of four. Limited ring inversion of the saddle-shaped porphyrin at low temperature may impose extra low symmetry on the system and double the number of peaks. Upon warming, while the resonances corresponding to phenyl protons get sharper, these four methylene peaks broaden and coalesce at about 100 °C. Above the coalescence temperature, two methylene signals grow back at 23.5 and 29.3 ppm. These variable-temperature NMR data

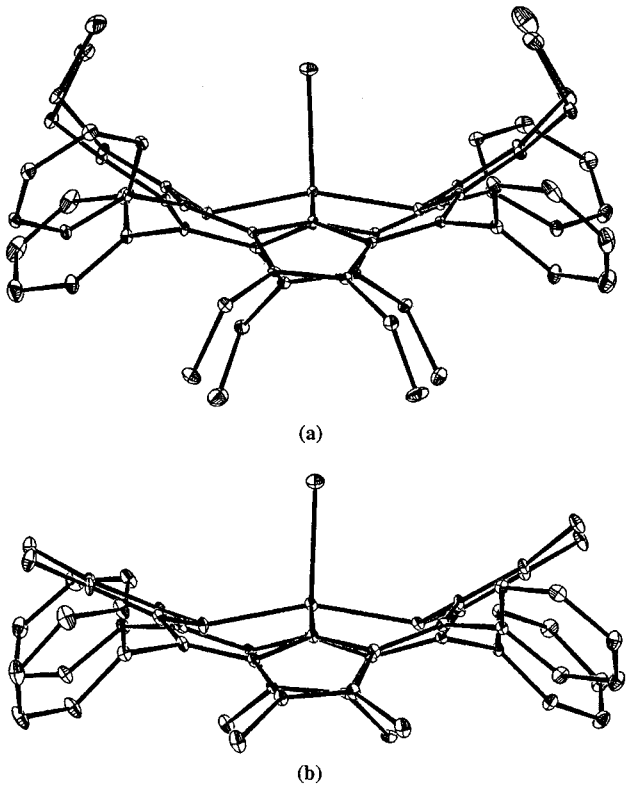

Figure 2. Perspective views of (a) Fe(OETPP)Cl and (b) Fe(OMTPP)-Cl that illustrate the deformations of the porphyrin skeletons and the orientations of substituents.

confirm that Fe(OETPP)Cl retains the saddle-shaped conformation in solution. The coalescence temperature, T_c, can be used to estimate the free energy of activation for the methylenes to become equivalent by using the standard equation, $\Delta G^{\ddagger}/RT_c = 22.96 + ln(T_c/\delta\nu)$,[13] where $\delta\nu$ is the difference in the methylene resonances extrapolating to T_c which can be obtained easily from the corresponding Curie plot. For a coalescence temperature of 373 K and $\delta\nu$ of 1875 Hz, this yields a value of $\Delta G^{\ddagger} = 15.8$ kcal/mol very close to the value obtained for Zn(OETPP)(py).[7]

Patterns of the paramagnetic NMR shifts of ferric porphyrins have been shown to be diagnostic of the iron spin state.[14] But in the case of highly substituted Fe(OETPP)Cl, without the more sensitive *meso*- and *pyrrole*-protons, the pattern of the spectrum is not very conclusive for the assignment of the spin state of the complex. Chemical shifts of methylene protons cover the range for high-spin Fe^{III}(OEP)Cl and intermediate-spin Fe^{III}-(OEP)($OClO_3$).

Variable-temperature ^{1}H NMR spectra of Fe(OMTPP)Cl taken in CD_2Cl_2 are very similar to that of Fe(OETPP)Cl in the phenyl resonance region. But there is only one methyl resonance near room temperature. It's our expectation that, there should be two methyl resonances corresponding to methyl groups *syn*- and *anti*- to the axial ligand in the saddle-shaped five coordinated Fe(OMTPP)Cl. Cooling down the sample did make the single methyl resonance split into two (ca. 71.2 and 80.7 ppm at −70 °C). This temperature dependence phenomenon suggests that Fe(OMTPP)Cl also retains the saddle-shaped conformation in solution but undergoes fast ring inversion near room temperature. For a coalescence temperature of 243 K and $\delta\nu$ of 1742 Hz (extrapolated from the corresponding Curie plot),

(13) Abraham, R. J.; Fisher, J.; Loftus, P. *In Introduction to NMR Spectroscopy*; Wiley and Sons: Chichester, England, 1988.

(14) Goff, H. M. In *Iron Porphyrins*; 1st ed.; Lever, A. B. P., Gray, H. B., Eds.; Addison-Wesley Publishing Company, Inc.: Reading, MA, 1983; Vol. 1; pp 237−281.

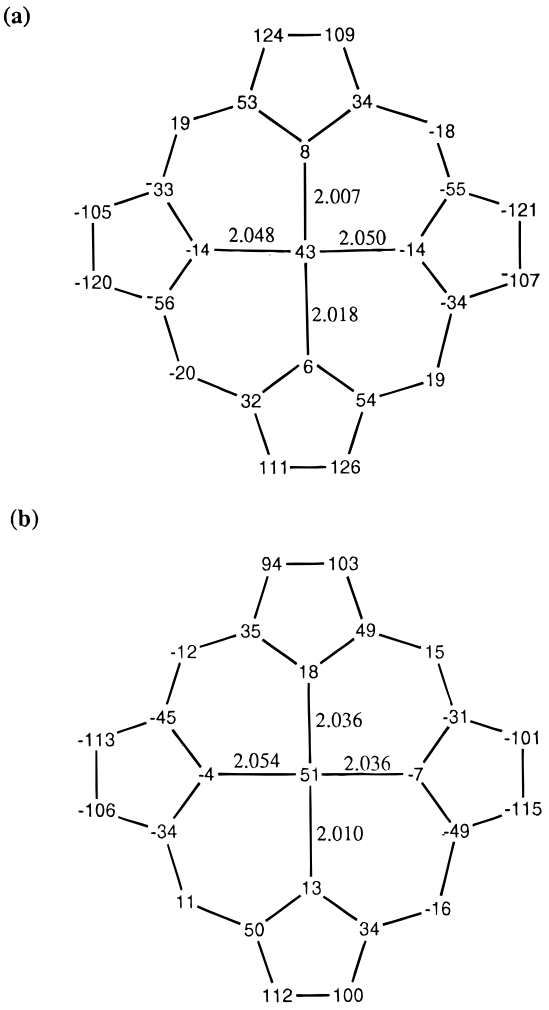

Figure 3. Formal diagrams of the porphyrin core of (a) Fe(OETPP)-Cl and (b) Fe(OMTPP)Cl, showing displacements of the 24 atoms from the mean plane of the 24 atoms (in units of 0.01 Å) and the Fe−N_p bond distances (in units of 1 Å).

this yields a value of $\Delta G^{\ddagger} = 10.1$ kcal/mol which is significantly smaller than the value of Fe(OETPP)Cl. Crystal structural data indicate that there is a small amount of difference of distortion between OETPP and OMTPP systems, but it's surprising to see such a large difference of activation energy for ring inversion.

Magnetic Measurements. Magnetic susceptibilities measured for Fe(OETPP)Cl at room temperature give the effective magnetic moments, μ_{eff}, of 5.1 and 5.2 μ_B in solution and on a microcrystalline sample, respectively. This value is too low for high spin (5.9 μ_B) and too high for intermediate spin (3.9 μ_B) assignment. The Curie−Weiss plot of Fe(OETPP)Cl illustrated in Figure 5a is not strictly linear. The amount of curvature is insufficient to be indicative of a thermal spin state equilibrium, but it does suggest that a simple $S = 3/2$ or 5/2 state is an inadequate description of the situation.[15] The temperature dependence of the magnetic moment shown in Figure 5b is very similar to the well established Fe(OEP)-($OClO_3$) and Fe(TPP)($OClO_3$) complexes which have been fully characterized to be a quantum mechanically mixed $S = 3/2$, 5/2 state remarkably similar to that of certain low-temperature cytochrome c'.[16,17]

(15) Reed, C. A.; Mashiko, T.; Bentley, S. P.; Kastner, M. E.; Scheidt, W. R.; Spartalian, K.; Lang, G. *J. Am. Chem. Soc.* **1979**, *101*, 2948−2958.

(16) Mitra, S. In *Iron Porphyrins*; 1st ed.; Lever, A. B. P., Gray, H. B., Eds.; Addison-Wesley Publishing Company, Inc.: Reading, MA, 1983; Vol. 2; pp 1−42.

(17) Maltempo, M. M. *J. Chem. Phys.* **1974**, *61*, 2540−2547.

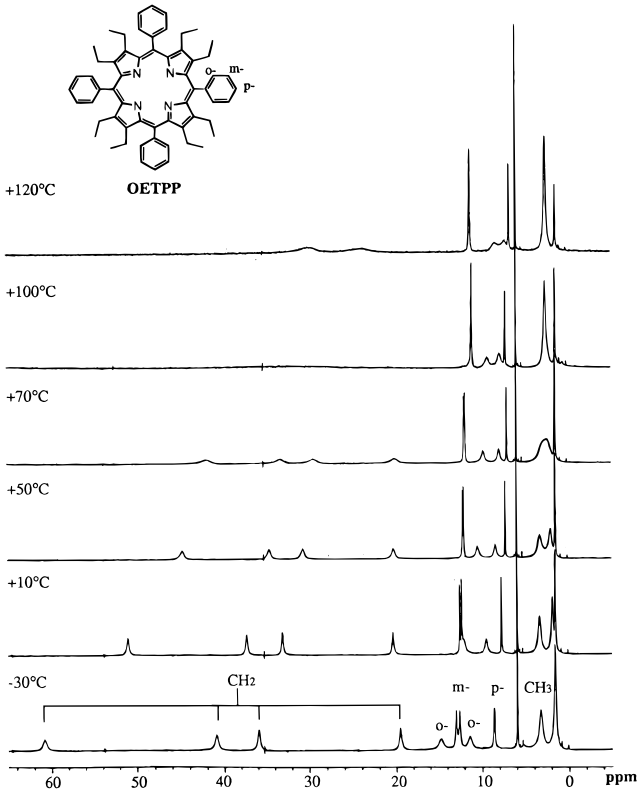

Figure 4. Variable-temperature 300 MHz proton NMR spectra of Fe-(OETPP)Cl taken in $C_2D_2Cl_4$.

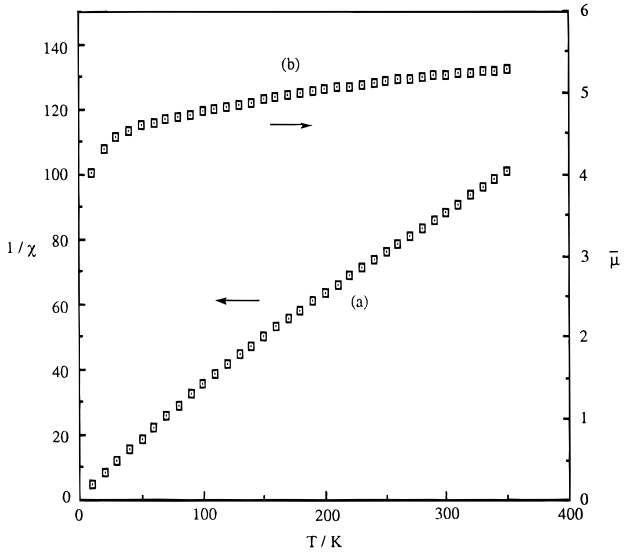

Figure 5. (a) Curie−Weiss plot and (b) temperature dependence of magnetic moment for Fe(OETPP)Cl.

Fe(OMTPP)Cl shows almost identical temperature-dependent magnetic properties as Fe(OETPP)Cl with μ_{eff} of 5.1 μ_B in the solid state at room temperature. Evans method magnetic susceptibility on Fe(OMTPP)Cl in $CDCl_3$ gives somewhat lower μ_{eff} of 4.7 μ_B.

Electron Paramagnetic Resonance. Further evidence for the quantum mechanically-mixed intermediate-spin state comes from EPR spectrum. The EPR spectrum of Fe(OETPP)Cl taken in 2-methyltetrahydrofuran at 77 K[18] shows a nearly axial symmetric $g_\perp = 5.2$ and $g_\parallel = 2.0$ (Figure 6). The apparent $g_\perp$

(18) Fe(OETPP)Cl and Fe(OMTPP)Cl show similar UV/vis and EPR spectra both in CH_2Cl_2 and 2-methyltetrahydrofuran. But the EPR signals are better resolved in 2-methyltetrahydrofuran. 2-Methylhydrofuran has been known to form good glasses at low temperature.

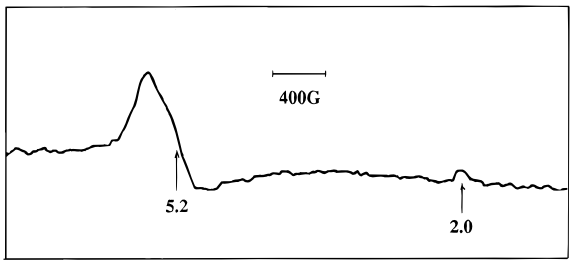

Figure 6. EPR spectrum of Fe(OETPP)Cl taken in 2-methyltetrahydrofuran at 77 K.

value is quite deviated from the range of typical high-spin ferric heme ($g_\perp = 6$) and the value predicted for intermediate-spin iron(III) porphyrin ($g_\perp = 4$).[16,17] On the basis of the model due to Maltempo, these two different spin states ($^6A_1$ and $^4A_2$) can be mixed quantum mechanically by spin-orbit coupling and can substantially modify the magnetism. A quantum mechanically admixed-spin system will give rise to a single set of EPR signals which is the average of the two participating spins. The theory is immediately applicable to our derivative with $g_\perp = 5.2$ giving rise to an $S = 5/2$ state with approximately 40% $S = 3/2$ admixture. Actually, the broad $g_\perp$ feature with additional shoulder is similar to the spectra of cytochromes *c*′ from *Rb. capsulatus* and *Rps. palustris* measured at 6 K which have also been estimated to be of about 60% high-spin state and 40% intermediate-spin state.[19]

The EPR spectrum of Fe(OMTPP)Cl taken in 2-methyltetrahydrofuran at 77 K with $g_\perp = 5.3$ and $g_\parallel = 2.0$ can be interpreted as a quantum-mixed intermediate-spin state with approximately 65% $S = 5/2$ and 35% $S = 3/2$.

Discussion

Structural and Crystal Field Basis for Heme Iron Spin State. Both the results from magnetic measurements and electron pramagnetic resonance spectroscopy illustrate that different from the normal high-spin Fe^{III}(OEP)Cl and Fe^{III}(TPP)Cl ($S = 5/2$) complexes, Fe^{III}(OETPP)Cl and Fe^{III}(OMTPP)Cl are of the uncommon quantum-mixed $S = 5/2$, 3/2 intermediate-spin very close to Fe^{III}(OEP)($OClO_3$) and Fe^{III}(TPP)($OClO_3$) complexes. Additional support for this unusual quantum-mixed intermediate-spin state came from the comparison of structural data of related complexes as summarized in Table 3. Bond length between Fe and porphinato nitrogen should be most sensitive to the nature of the central iron. The value Fe−N_p of 2.03 Å for both Fe(OMTPP)Cl and Fe(OETPP)Cl is significantly shorter than 2.07 Å for high-spin Fe(TPP)Cl. This is consistent with the depopulation of $d_{x^2-y^2}$ orbital for a quantum-mixed intermediate-spin state. Other structural parameters important for identifying the spin state of five-coordinate ironporphyrins are the displacement of the iron atom from the mean plane of the 24-atom core (Ct_p) or the mean plane of the four nitrogen atoms (Ct_N). The values Fe−Ct_p of 0.43 and 0.51 Å and the values Fe−Ct_N of 0.47 and 0.46 Å for Fe(OETPP)Cl and Fe(OMTPP)Cl respectively are smaller than Fe−Ct_p of 0.57 Å and Fe−Ct_N of 0.49 Å for Fe(TPP)Cl. These results are also in the right direction for the change of spin state. The difference between Fe−Ct_p and Fe−Ct_N is related to C_{4v} doming of five-coordinate metalloporphyrins. Fe(OETPP)Cl shows an unusual feature of reverse doming (Fe−Ct_p < Fe−Ct_N). It is important to emphasize that saddle-shaped ring deformation may impose extra changes to the coordination sphere of the central metal.[9] Whether it's appropriate to compare the structural parameters directly between nonplanar and planar porphyrins must await further systematic structural studies.

In summary, two new quantum-mixed intermediate-spin iron(III) porphyrin complexes, Fe(OETPP)Cl and Fe(OMTPP)Cl, with a different amount of mixing of the spin sextet state have been recognized. An argument which arises from crystal field theory for a tetragonal system suggests that the choice between an $S = 5/2$ and $S = 3/2$ spin state is directly governed by the energy separation between $d_{x^2-y^2}$ and the nearly degenerate d_{xy}, d_{xz}, d_{xz} orbitals. This implies that no relatively stable quartet state should be found without changing the basic iron-porphyrin coordination. While the smaller "hole" of the phthalocyanines[20,21] and tetraazaporphyrin[22] splits the iron d orbitals to a greater extent than does a porphyrin, resulting in a lower spin ($S < 5/2$) complex, the saddle-shaped ring deformations of OETPP and OMTPP increase the σ donor abilities of the porphyrin macrocycles and further destabilize the $d_{x^2-y^2}$ orbital, thereby leading to a natural way to stabilize the intermediate-spin state. While both Fe(OEP)Cl and Fe(TPP)Cl are typical high-spin complexes, just by twisting the conformation of the macrocycle without changing the axial ligand, Fe(OETPP)Cl and Fe(OMTPP)Cl will show properties with mixed intermediate-spin state.

To the best of our knowledge, all the intermediate-spin iron(III) porphyrin systems reported up to now were controlled by the axial ligand field strength (e.g., ClO_4^-, $CF_3SO_3^-$, and $C(CN)_3^-$ etc.)[15,23−27] or in one case controlled by the axial ligand orientation.[2] There is a unique example of a pure intermediate-spin Fe(III) porphyrin complex with a vinylidene carbene inserted into an Fe−N bond of a highly disturbed porphyrin macrocycle.[28] This perturbation obviously reduces the symmetry and imposes a large magnetic anisotropy to the system.

Studies of model heme compounds show that the intermediate-spin state depends critically on the presence of a weak field axial ligand. Perturbation of the ligand field in the axial direction (*z*) may only affect the the splitting of d orbitals in the equatorial (*x*, *y*) plane indirectly. As the *z* axis ligand decreases its charge interaction with the iron atom, a compensating increase in attraction of the equatorial ligands will occur. The radial contraction of a porphyrin is significant and illustrated by the structural comparison of high-spin Fe(TPP)Cl with the intermediate-spin Fe(TPP)($OClO_3$) as shown in Table 3. The concomitant decrease of the Fe−N_p bond length in the xy plane should cause an increase of the Fe−A_x bond length which could not be checked in the model system with different axial ligands.

The way ring-deformation modulates the splitting of d orbitals is from the opposite direction. Increase of the *xy* crystal field of the porphyrin ligand initiates the perturbation and results in weakening of the crystal field in the *z* axis. This is evident by the structural comparison of high-spin Fe(TPP)Cl with inter-

(19) Fujii, S.; Yoshimura, T.; Kamada, H.; Yamaguchi, K.; Suzuki, S.; Shidara, S.; Takakuwa, S. *Biochim. Biophys. Acta.* **1995**, *1251*, 161−169.
(20) Kennedy, B.; Brain, G.; Murray, K. *Inorg. Chim. Acta.* **1984**, *81*, L29−L31.
(21) Kennedy, B.; Murray, K.; Zwack, P.; Homborg, H.; Kalz, W. *Inorg. Chem.* **1986**, *25*, 2539−2545.
(22) Fitzgerald, J. P.; Haggerty, B. S.; Rheingold, A. L.; May, L. *Inorg. Chem.* **1992**, *31*, 2006−2013.
(23) Boersma, A. D.; Goff, H. M. *Inorg. Chem.* **1982**, *21*, 581−586.
(24) Goff, H.; Shimomura, E. *J. Am. Chem. Soc.* **1980**, *102*, 31−37.
(25) Masuda, H.; Taga, T.; Osaki, K.; Sugimoto, H.; Yoshida, Z.-I.; Ogoshi, H. *Inorg. Chem.* **1980**, *19*, 950−955.
(26) Dolphin, D. H.; Sams, J. R.; Tsin, T. B. *Inorg. Chem.* **1977**, *16*, 711−713.
(27) Gismelseed, A.; Bominaar, E. L.; Bill, E.; Trautwein, A. X.; Winkler, H.; Nasri, H.; Doppelt, P.; Mandon, D.; Fischer, J.; Weiss, R. *Inorg. Chem.* **1990**, *29*, 2741−2749.
(28) Mansuy, D.; Morgenstern-Badarau, I.; Lange, M.; Gans, P. *Inorg. Chem.* **1982**, *21*, 1427-1430.

Table 3. Stereochemical/Spin-State Relationships in Iron(III) Porphyrin complexes

	Fe(TPP)Cl	Fe(OMTPP)Cl	Fe(OETPP)Cl	Fe(TPP)($OClO_3$)	Fe(OEP)($OClO_3$)
Fe−N_p (Å)[a]	2.070(9)	2.034(6)	2.031(5)	2.001(5)	1.994(10)
Fe−C_{tp} (Å)[b]	0.59	0.51	0.43	0.30	0.26
Fe−C_{tN} (Å)[c]	0.49	0.46	0.47	0.28	0.26
C_{tN-Np} (Å)	2.011[d]	1.980	1.978	1.981	1.977
Fe−A_x (Å)[e]	2.211(1)	2.247(3)	2.2418(23)	2.029(4)	2.067(9)
$_{eff}$ (μ_B)	5.9 (300 K)	4.7−5.1 (300 K)	5.1−5.2 (300 K)	5.2 (300 K)	4.8 (275 K)
$g_\perp$	6.0	5.3	5.2	4.75	4.37
g_{ll}	2.0	2.0	2.0	2.03	2.00
spin state	h.s.	admixed i.s.	admixed i.s.	admixed i.s.	admixed i.s.
$S = 3/2$	0%	35%	40%	65%	82%
$S = 5/2$	100%	65%	60%	35%	18%
ref	12, 16	this work	this work	15, 16	26, 16

[a] N_p, porphinato nitrogen. [b] $C_{tp,}$ center of the best plane of the 24-atom porphinato core. [c] $C_{tN,}$ center of the best plane of the four N_p. [d] Estimated from $(C_{tN}-N_p)^2 = (Fe-N_p)^2 - (Fe-C_{tN})^2$. [e] A_x, axial ligand donor atom.

mediate-spin Fe(OETPP)Cl and Fe(OMTPP)Cl, where the Fe−Cl distances are 0.03 Å longer in the intermediate-spin complexes.

Electronic Structure Asymmetry. Other than the number of peaks of methylene protons, there is another feature in the ^{1}H NMR spectrum of Fe(OETPP)Cl. Those resonances corresponding to the four methylene protons spread out in a large range of more than 20 ppm at room temperature. Similar large asymmetry of ring-methyl shifts has been reported for the hemoprotein. These unusual shifts of certain resonances in the proton NMR spectra of heme proteins have been explained by the peripherial effects from hydrogen-bonding solvent or protein contacts and the spatial orientation of planar imidazole ligand.[14,29] However, with our model system, none of these rationalizations are applicable. It is our expectation that the unusually large spread of signals for the methylene protons of Fe(OETPP)Cl can only be explained by the following two factors. (i) The geometric factor of the out of plane location of the central iron in combination with the saddle-shaped porphyrin ring deformation. This spatial arrangement will make those methylene protons that tilt toward and away from the single axial ligand have different distances from iron and suffer different extents of paramagnetic shifts from the metal center. (ii) Lifting of the degeneracy of the d_{xz} and d_{yz} orbitals will occur by the same conformation effect. Saddle-shaped deformation of porphyrin macrocycle for a five-coordinate metal complex will lower the symmetry of the metal site into C_{2v}. This low symmetry should split d_{xz} and d_{yz} orbitals into b_1 and b_2 sublevels. These sublevels may have different amounts of interaction with the porphyrin macrocycle and result in different spin densities along *x* and *y* axes. This anisotropic electronic state may induce a large asymmetry to the peripheral methylene proton shifts, as is further confirmed by the rhombic symmetry of EPR signals. The alternative two long and two short pattern of Fe−N_p bond distances along two different axes (Figure 3) also supports the second argument.

Models of Cytochrome *c*′. At physiological pH, the bacterial heme proteins known as the ferric cytochromes *c*′ have magnetic properties and EPR spectra unlike those of typical high-spin or low-spin ferric heme proteins. Maltempo suggests that this class of heme proteins can be accounted for by a ground state heme-iron electronic configuration which is a unique quantum mechanical admixture of an intermediate-spin state ($S = 3/2$) and a high-spin state ($S = 5/2$).[16,17] Interestingly the contribution of the intermediate-spin state ($S = 3/2$) to the ground state depends upon pH, temperature, and the bacterial source from which cytochrome *c*′ is derived.[19]

The heme iron in cytochromes *c*′ is pentacoordinate and is displaced from the mean heme plane toward the fifth ligand histidine. Based on previous model complex studies of Fe(TPP)X (X = ClO_4^-, $CF_3SO_3^-$, and $C(CN)_3^-$ etc.), it has been suggested that protein-induced histidine constraint (e.g., hydrogen-bonding to the imidazole side-chain) which slightly lowered its ligand field strength may be responsible for the unusual spin state of cytochrome *c*′ and would be consistent with the high sensitivity of the spin state of cytochrome *c*′ to its enviroment.[15,30] In model studies, there is a clear correlation between spin state of the heme iron and the Fe−Ct distances which in turn will affect the axial ligand field strength.[19] However, previous X-ray studies of these ferric cytochromes *c*′ isolated from corresponding bacteria do not follow this pattern.[19,31,32,30] On the other hand, while most of the EPR spectra of model porphyrin complexes previously reported have been analyzed as axially symmetric, the spectra of the protein can only be simulated with rhombic *g* tensors and highly anisotropic line widths.[19] These discrepancies can be eliminated in our nonplanar model system, where the spin state of heme iron is correlated with the deviation of the porphyrin macrocycle from planarity, and the characteristic rhombic symmetry is a natural result of the C_{2v} point group.

It has always been overlooked that all the protein structural data of these ferric cytochromes *c*′ indicate a small but definite saddle-shaped distortion from planarity for the heme.[31,32,30] Similar but larger ring deformations of some photosynthetic chromophores have been demonstrated to be imposed by protein constraints.[4] Based on the structural and spectral similarity between our model system and ferric cytochrome *c*′ from photosynthetic bacteria, it is reasonable to propose that ring deformation instead of axial ligand field strength may be the main mechanism to mediate the electronic structure of this series of heme proteins. Nevertheless, it's our expectation that cytochrome *c*′ would have a larger degree of distortion in solution at physiological pH than it does in solid state in order to show a significant change of spin state. This point may be checked by taking EPR spectra for ferric cytochrome *c*′ in the polycrystalline form.

Conclusion

Similar to other metalloporphyrin complexes of OETPP and OMTPP, Fe(OETPP)Cl and Fe(OMTPP)Cl are both clearly saddle-shaped with the former more distorted than the latter.

(29) Zhang, H.; Simonis, U.; Walker, F. A. *J. Am. Chem. Soc.* **1990**, *112*, 6124−6126.

(30) Finzel, B. C.; Weber, P. C.; Hardman, K. D.; Salemme, F. R. *J. Mol. Biol.* **1985**, *186*, 627−642.

(31) Ren, Z.; Meyer, T.; McRee, E. *J. Mol. Biol.* **1993**, *234*, 433−445.

(32) Yasui, M.; Harada, S.; Kai, Y.; Kasai, N.; Kusunoki, M.; Matsuura, Y. *J. Biochem.* **1992**, *111*, 317−324.

Nonplanar deformation of the porphyrin macrocycle can induce a change of spin state and a large spread of the NMR signals, which to our knowledge have not been previously reported. And most of all, certain cytochromes *c*′ from photosynthetic bacteria, reported to be of similar quantum-mixed intermediate-spin and showing EPR signals of rhombic symmetry, have been noted to have saddle-shaped deformations. Based on the structural and spectral similarity between our model system and ferric cytochrome *c*′ from photosynthetic bacteria, we are confident that ring deformation may be the novel mechanism which mediates the electronic structure of this series of heme proteins. The relevance of this observation is obvious when one considers the importance of the spin state for biological activities in heme proteins. The actual functional consequences of this spin state change in various proteins offer new insights into the importance of ring conformation in model heme complexes.

Acknowledgment. This work was supported by the National Science Council of the Republic of China, Grant No. NSC83-0208-M005-049 and NSC85-2113-M005-018.

Supporting Information Available: Tables of final fractional atomic coordinates and anisotropic thermal parameters for the non-hydrogen atoms, final positional parameters for the hydrogen atoms, complete bond distances, and bond angles for Fe(OETPP)Cl and Fe(OMTPP)Cl, variable-temperature 300 MHz proton NMR spectra of Fe(OMTPP)Cl taken in CD_2Cl_2, Curie plots of proton resonances of Fe(OETPP)Cl and Fe(OMTPP)Cl, and Curie−Weiss plot and temperature dependence of magnetic moment for Fe(OMTPP)Cl (18 pages). See any current masthead page for ordering and Internet access instructions.

JA962474X